Accelerated Arctic land warming and permafrost degradation during rapid sea ice loss

David M. Lawrence[1], Andrew G. Slater[2], Robert A. Tomas[1], Marika M. Holland[1], Clara Deser[1]

[1]*Climate and Global Dynamics Division, National Center for Atmospheric Research*

[2]*Cooperative Institute for Research in Environmental Sciences*
University of Colorado, Boulder, Colorado

Submitted to Geophysical Research Letters
March 7, 2008

Corresponding Author:

David M. Lawrence
NCAR/CGD
P.O. Box 3000
Boulder, CO 80307

Tel: 303-497-1384
Fax: 303-497-1348
Email: dlawren@ucar.edu

Abstract

Coupled climate models and recent observational evidence suggest that Arctic sea ice may undergo abrupt periods of loss within fifty years. Here, we evaluate the impact of rapid sea ice loss on terrestrial Arctic climate and ground thermal state in the Community Climate System Model. We find that western Arctic land warming trends during rapid sea ice loss are 3.5 times greater than secular 21st century climate-change trends outside these periods. The accelerated warming signal extends up to 1500km inland and is apparent throughout most of the year, peaking in autumn. Idealized experiments using the Community Land Model, with improved permafrost dynamics, indicate that an accelerated warming period substantially increases ground heat accumulation – the earlier the event the greater the long-term impact. For warm permafrost, enhanced heat accumulation can lead to rapid degradation. For colder ground, heat accumulation preconditions permafrost for earlier and/or more rapid degradation under continued warming.

1. Introduction

Over the past several decades, Arctic sea ice extent has been steadily shrinking. Due to the ice-albedo feedback, this reduction in ice cover has contributed to an observed amplification of Arctic warming [*Serreze and Francis*, 2006]. In general, Arctic sea ice area is a robust inverse predictor of Arctic land air temperature (T_{air}). Over the period 1979 to 2006, June to September detrended sea ice area (data from [*Stroeve and Meier*, 1999]) and detrended western Arctic land air temperature (65°-80°N, 90°-270°E; data from Climate Research Unit, CRUTEM3 [*Jones et al.*, 2006]) are correlated at −0.59 ($P < 0.01$).

In September 2007, the annual minimum sea ice extent shattered the previous observational-record low [*Stroeve et al.*, 2008]. Preliminary CRUTEM3 data indicate that 2007 August to October western Arctic land temperatures were the warmest of the last 30 years (+2.3°C warmer than the 1978 to 2006 average). The striking sea ice decline in 2007 raises the specter that a period of abrupt sea ice loss, such as those simulated in Community Climate System Model (CCSM3) 21st century A1B simulations [*Holland et al.*, 2006b], is a distinct possibility. Rapid sea ice loss events (RILEs) in CCSM3 typically last between 5 and 10 years and exhibit negative sea ice extent trends that are roughly 4 times larger than average simulated (or recently observed) trends. Analogous abrupt sea ice loss events are found in roughly 50% of the Intergovernmental Panel on Climate Change Fourth Assessment Report (IPCC AR4) coupled models. CCSM3 exhibits both a reasonable simulation of present-day sea ice conditions (extent

and thickness) and replicates the rate of sea ice loss over the last few decades [*Holland et al.*, 2006a].

Whether or not the 2007 sea ice record minimum is a precursor of a sustained period of rapid loss remains to be seen, but the record provides motivation to assess the potential consequence for adjacent land climate. Here, we evaluate Arctic land temperature response to RILEs in CCSM3. We find that the secular 21st century land warming trend is augmented by a factor of 3.5 during RILEs, which is likely to have adverse impacts on permafrost. Through idealized experiments with the Community Land Model (CLM), we assess the impact of a RILE and its timing on permafrost.

2. Arctic land temperature trends during rapid sea ice loss events

Nine RILEs are identified across the eight member CCSM3 A1B 21st century ensemble [*Holland et al.*, 2006b]. By computing a lagged composite of sea ice extent anomalies across the nine events, we form a picture of the typical sea ice extent trajectory during abrupt loss periods (Fig. 1a). A corresponding composite for western Arctic October to December (OND) land T_{air} shows an increase in warming during RILEs (Fig. 1a). Figure 1b shows the western Arctic linear T_{air} trend during and outside RILEs. Warming is accelerated during RILEs throughout most of the year with statistically significant increases in warming rates apparent in the summer and early autumn, likely due to increased open water area, as well as in late autumn and winter, when the thinner ice pack less efficiently insulates the atmosphere from the comparatively warm ocean water below. Accelerated warming spans most of the terrestrial western Arctic juxtaposed to

98 the area of sea ice contraction in CCSM3. It is strongest along the Arctic coast where it
99 is as high as 5°C decade^{-1} in the autumn, but a signal of enhanced warming can extend
100 1500 km inland (Fig. 1c). Annually averaged, the warming trend during RILEs is 3.5
101 times greater than outside these periods (1.60°C decade^{-1} versus 0.46°C decade^{-1}).
102
103 Corresponding analyses are performed for precipitation (P), snow depth, specific
104 humidity (q_{air}), and downwelling longwave (LW↓) and solar (SW↓) radiation. Relative
105 humidity (RH) remains roughly constant with warming and consequently specific
106 humidity and LW↓ exhibit accelerated trends in harmony with T_{air}. Trends during RILEs
107 for snow depth, P, and SW↓ are not statistically differentiable from the secular 21st
108 century trends for these quantities.
109
110 The acceleration in Arctic land warming during RILEs raises an obvious question as to
111 whether or not accelerated warming is predominantly a response to, rather than a forcing
112 of, rapid sea ice loss. *Holland et al.* [2006b] argue that abrupt sea ice transitions are
113 thermodynamically driven with enhanced open water production, as ice thins, leading to
114 more solar radiation absorbed. An episodic increase in ocean heat transport to the Arctic,
115 and associated ice thinning, may act as a trigger for abrupt ice loss. Rising T_{air} is not
116 cited as a principal triggering mechanism.
117
118 The intuitive interpretation that warming over land is a response to sea ice loss is
119 supported by a set of atmosphere-land simulations that isolate the influence of future
120 versus present-day sea ice conditions on climate (e.g. separate from greenhouse gas

121 forcing). Two 60-yr simulations with the Community Atmosphere Model (CAM3,
122 [*Collins et al.*, 2006b]) coupled to CLM3 were conducted. The first simulation is forced
123 with monthly average sea ice thickness and distribution from CCSM3 for the years 1980-
124 1999. The second simulation uses the thinner and contracted sea-ice conditions from
125 CCSM3 A1B integrations for the years 2080-2099. Both simulations use the same
126 observed climatological sea surface temperatures. Differences in T_{air} due to sea ice loss
127 show a pattern of warming (Fig. 2) that is consistent with the pattern of accelerated
128 warming during rapid sea ice retreat in the fully coupled integrations (Fig. 1c). The
129 annual cycle phase of the warming is also similar with the strongest warming occurring in
130 autumn and early winter.

131 ## 3. Impact of accelerated warming on permafrost
132

133 a. Community Land Model

134

135 CLM3.5 [*Oleson et al.*, 2008] is a state-of-the-art process-based model of the land-
136 surface that serves as the land component of the CCSM3 [*Collins et al.*, 2006a]. It
137 calculates heat and radiation fluxes at the land-atmosphere interface, as well as
138 temperature, humidity, and soil thermal and hydrologic states – including explicit
139 treatment of soil freeze/thaw processes. The 5-layer snow model represents processes
140 such as accumulation, melt, compaction, ageing, and water transfer across layers.
141 Improvements over CLM3.5 include explicit representation of the thermal and hydrologic
142 properties of organic soil [*Lawrence and Slater*, 2007] and a 50m soil column that
143 represents thermal inertia provided by deep ground [*Lawrence et al.*, 2008]. Given

144 observed forcing, this version of the model reasonably simulates observed soil
145 temperature-depth-annual cycle relationships for tested locations in Siberia and Alaska
146 [*Nicolsky et al.*, 2007; *Lawrence et al.*, 2008]. To focus in on the detailed response of
147 near-surface permafrost to warming, we increase soil vertical resolution 4-fold from 15 to
148 60 layers. Layer thicknesses range from a minimum of 1.5cm at the surface to 29cm at
149 3m depth to 390cm at column bottom.
150
151 b. Synthetic Arctic climatic trend scenarios
152
153 In the CCSM3 A1B ensemble, RILEs initiate at years ranging from 2012 to 2045, with
154 one ensemble member not exhibiting an abrupt event. Here, we construct four synthetic
155 T_{air} trend scenarios that reflect the range of possibilities for an abrupt event with 10-yr
156 long accelerated warming periods occurring early (yrs 6-15, EARLY), in the middle (yrs
157 21-30, MID), or in the latter part (yrs 36-45, LATE) of a 50-yr period, or not at all
158 (LINEAR) (see Table 1, Fig. 3a). Monthly T_{air} anomaly time series are constructed
159 based on the calculated CCSM3 trends during and outside RILEs (Fig. 1b) by recursively
160 adding the monthly trend (°C yr^{-1}) year after year in the following manner, for example
161 for the EARLY scenario,

162 $$T_{air}(m,y) = T_{air}(m,y-1) + \Delta T_{avg}(m) \qquad y = 1,2,3,4,5$$

163 $$T_{air}(m,y) = T_{air}(m,y-1) + \Delta T_{accel}(m) \qquad y = 6,7,8,...15$$

164 $$T_{air}(m,y) = T_{air}(m,y-1) + \Delta T_{avg}(m) \qquad y = 16,17,18,...50$$

where m is the month (m = 1,2,3, … 12), y is the year, and ΔT_{avg} and ΔT_{accel} are the monthly T_{air} trends as in Fig. 1b. For the LINEAR scenario,

$$T_{air}(m,y) = T_{air}(m,y-1) + \frac{4\Delta T_{avg}(m) + \Delta T_{accel}(m)}{5} \qquad y = 1,2,3,...50 .$$

The annual mean temperature change at year 50 is exactly the same for each scenario (+3.5°C).

We also adjust q_{air} so that RH is conserved as T_{air} rises. Since LW↓ is a function of T_{air} and q_{air}, their modification influences LW↓ forcing. Hence, the accumulated LW↓ anomaly is highest in EARLY, while it is exactly the same in LINEAR and MID (Fig. 3b). Due to the lack of statistically significant alterations in P or SW↓ trends during RILEs, we do not apply trends for these quantities. These experiments, therefore, are idealized and are designed to focus on the impact of accelerated warming in the absence of other climate perturbations. CCSM3 and most other GCMs project that the high-latitudes will become wetter and cloudier during the 21st century [*IPCC*, 2007]. The actual rate of soil warming will be due to the combined changes in T_{air}, P, snow depth, and other forcings (e.g. vegetation, SW↓, disturbance, etc.).

For each synthetic warming scenario, 50-yrs of gridded forcing data are created by adding T_{air}, q_{air}, and LW↓ anomalies to observed 3-hourly time series from an arbitrary year. Prior to integrating the model with the synthetic trend scenarios, CLM is spun-up for 400 years with repeat year 2000 forcing data [*Qian et al.*, 2006].

186

187 c. Results from warming scenario experiments

188

189 The impact of accelerated warming is shown for three illustrative ground conditions
190 representing differing initial permafrost states (warm to cold) (Figs. 3c and 3d). These
191 cases all exhibit minimal snow depth change (< 10%) over the 50-yr simulation. For
192 initially cold permafrost, the timing of accelerated warming has little influence on the rate
193 of active layer deepening. All four scenarios simulate an ~0.35m deepening of the active
194 layer (Table 1). However, the soil heat content (SHC) gained in EARLY (191 MJ m^{-2}) is
195 30% larger than in LATE (147 MJ m^{-2}). The additional heat gained in EARLY
196 corresponds to +0.41°C more warming over the 50m column. For reference, this SHC
197 difference due to the timing of accelerated warming is almost two-thirds the 70MJ m^{-2}
198 estimated global average land heat gain for the period 1950 to 2000 [*Beltrami et al.*,
199 2002]. The SHC increase is 8% higher (+13 MJ m^{-2}, +0.11°C) in MID relative to
200 LINEAR even though accumulated LW↓ is the same in both.

201

202 For warm permafrost, the timing of accelerated warming has a more dramatic influence.
203 In all four scenarios, DPT increases slowly at first but accelerates rapidly once a layer of
204 perpetually unfrozen ground forms above the permafrost table (talik) at ~2m depth. This
205 occurs much sooner in EARLY with accelerated warming instigating talik formation by
206 year 12. By year 50, the warm permafrost soil column in EARLY has absorbed 900 MJ
207 m^{-2}, 68% more than LATE, and the DPT is 3.6m deeper compared to only 1.9m deeper in
208 LATE. Accelerated warming in the middle of the simulation results in more heat gain

209 and leads to greater DPT deepening than when warming is linear, even though total LW↓
210 forcing is the same.

211 ## 4. Discussion
212
213
214 Why does talik formation coincide with a strong increase in SHC accumulation rates?
215 Taliks form when the downwelling summer heating wave extends deeper than the
216 corresponding winter cooling wave, thereby preventing the talik from refreezing in winter
217 (e.g., perpetually high SHC zone in Fig. 4). Near isothermal soil layers at 0°C beneath
218 the talik also limit cooling from below. At this point, with continued warming, heat
219 accumulates at the maximum depth of the heating wave and permafrost degrades rapidly.
220
221 In colder permafrost, where a talik does not form, the timing of the accelerated warming
222 is less critical. However, the additional SHC gained from near-term accelerated warming
223 period preconditions cold permafrost for earlier and/or more rapid degradation under
224 continued warming.
225
226 Recent observational evidence suggests that permafrost may be vulnerable to rapid
227 warming. *Jorgenson et al.* [2006] find a dramatic increase in permafrost degradation in
228 association with a 2° to 5°C warming in central Alaska over the period 1989-1998.
229 *Isaksen et al.* [2007] argue that large T_{air} anomalies, such as those recently observed on
230 Svalbard, are likely to hasten permafrost degradation.
231

232 An abrupt change in Arctic climate is likely to have additional impacts beyond those on
233 permafrost. Ecosystems, particularly sensitive ones such as those found in the Arctic,
234 may be vulnerable to rapid change. Arctic ecosystems are already displaying a
235 propensity for sudden change with recent observations indicating increased shrubbiness,
236 longer growing seasons, advancing treelines, shifting migratory bird ranges, and
237 declining caribou herd health [*Hinzman et al.*, 2005]. Positive feedbacks in the Arctic
238 system could amplify these changes [*McGuire et al.*, 2006]. Enhanced permafrost
239 degradation may itself alter tundra ecosystems and biogeochemical cycling through the
240 formation of thermokarst and the redistribution of surface water [*Jorgenson et al.*, 2006].
241 Lastly, rapid near-term permafrost degradation would have implications for infrastructure
242 planning.
243

244 ## 5. Summary
245

246 We find that rapid sea ice loss forces a strong acceleration of Arctic land warming in
247 CCSM3 (3.5-fold increase, peaking in autumn) which may trigger rapid degradation of
248 currently warm permafrost and precondition colder permafrost for subsequent
249 degradation under continued warming. This sea ice loss – land warming relationship may
250 be immediately relevant given the record low sea ice extent in 2007. Our results also
251 suggest that talik formation, due to accelerated warming, may be a harbinger of rapid
252 subsequent terrestrial change.
253
254

Acknowledgements

This research was supported by the Office of Science (BER), U. S. DOE, Cooperative Agreement No. DE-FC02-97ER62402 and NSF grants ARC-0229769 and ARC-0531040.

References

Beltrami, H., J. E. Smerdon, H. N. Pollack, and S. P. Huang (2002), Continental heat gain in the global climate system, *Geophys. Res. Lett.*, *8*, doi:10.1029/2001GL014310.

Collins, W. D., et al. (2006a), The Community Climate System Model Version 3 (CCSM3), *J. Clim.*, *19*, 2122-2143.

Collins, W. D., P. J. Rasch, B. A. Boville, J. J. Hack, J. R. McCaa, D. L. Williamson, B. P. Briegleb, C. M. Bitz, S.-J. Lin, and M. Zhang (2006b), The Formulation and Atmospheric Simulation of the Community Atmosphere Model Version 3 (CAM3), *J. Clim.*, *19*, 2144-2161.

Hinzman, L. D., et al. (2005), Evidence and implications of recent climate change in northern Alaska and other arctic regions, *Clim. Change*, *72*, 251-298.

Holland, M. M., C. M. Bitz, E. C. Hunke, W. H. Lipscomb, and J. L. Schramm (2006a), Influence of the sea ice thickness distribution on polar climate in CCSM3, *J. Clim.*, *19*, 2398-2414.

Holland, M. M., C. M. Bitz, and B. Tremblay (2006b), Future abrupt reductions in the summer Arctic sea ice, *Geophys. Res. Lett.*, *33*, L23503, doi:10.1029/2006GL028024.

IPCC (2007), *Climate Change 2007: The Physical Science Basis. Contribution of Working Group I to the Fourth Assessment Report of the Intergovernmental Panel on Climate Change*, [S. Solomon, D. Qin, M. Manning, Z. Chen, M. Marquis, K. B. Averyt, M. Tignor and H. L. Miller (eds.)], Cambridge University Press, Cambridge, United Kingdom and New York, NY, USA.

281 Isaksen, K., R. E. Benestad, C. Harris, and J. L. Sollid (2007), Recent extreme near-
282 surface permafrost temperatures on Svalbard in relation to future climate
283 scenarios, *Geophys. Res. Lett.*, *17*, L17502, doi:10.1029/2007GL031002.
284 Jones, P. D., D. E. Parker, T. J. Osborn, and K. R. Briffa (2006), Global and hemispheric
285 temperature anomalies--land and marine instrumental records. In Trends: A
286 Compendium of Data on Global Change. [Available online at
287 Jorgenson, M. T., Y. L. Shur, and E. R. Pullman (2006), Abrupt increase in permafrost
288 degradation in Arctic Alaska, *Geophys. Res. Lett.*, *25*, L02503,
289 doi:10:1029/2005GL024960.
290 Lawrence, D. M., and A. G. Slater (2007), Incorporating organic soil into a global
291 climate model, *Clim. Dyn.*, doi:10.1007/s00382-007-0278-1.
292 Lawrence, D. M., A. G. Slater, V. E. Romanovsky, and D. J. Nicolsky (2008), The
293 sensitivity of a model projection of near-surface permafrost degradation to soil
294 column depth and inclusion of soil organic matter, *In press J. Geophys. Res.*
295 McGuire, A. D., F. S. Chapin, J. E. Walsh, and C. Wirth (2006), Integrated Regional
296 Changes in Arctic Climate Feedbacks: Implications for the Global Climate
297 System, *Ann. Rev. Env. Resources*, *31*, 61-91.
298 Nicolsky, D. J., V. E. Romanovsky, V. A. Alexeev, and D. M. Lawrence (2007),
299 Improved modeling of permafrost dynamics in a GCM land-surface scheme,
300 *Geophys. Res. Lett.*, *34*, L08501, doi:10.1029/2007GL029525.
301 Oleson, K. W., et al. (2008), Improvements to the Community Land Model and Their
302 Impact on the Hydrological Cycle, *In press J. Geophys. Res.*

303 Qian, T., A. Dai., K. E. Trenberth, and K. W. Oleson (2006), Simulation of global land
304 surface conditions from 1948 to 2002: Part I: Forcing data and evaluations, *J.*
305 *Hydromet.*, *7*, 953-975.
306 Serreze, M. C., and J. A. Francis (2006), The arctic amplification debate, *Clim. Change*,
307 *76*, 241-264.
308 Stroeve, J., and W. Meier (1999), updated 2006. Sea Ice Trends and Climatologies from
309 SMMR and SSM/I. [Available online at
310 Stroeve, J., M. Serreze, S. Drobot, S. Gearhead, M. Holland, J. Maslanik, W. Meier, and
311 T. Scambos (2008), Arctic sea ice plummets in 2007, *EOS*, *89*, 13-14.
312
313

Table 1. Change in DPT and SHC from year 1 to year 50 for three representative initial permafrost states identified by annual mean T_{soil} at the permafrost table in year 1, $\overline{T_{soil}(PT, y=1)}$.

Experiment	Description	$\overline{T_{soil}(PT, y=1)}$ **−0.3°C**		$\overline{T_{soil}(PT, y=1)}$ **−1.5°C**		$\overline{T_{soil}(PT, y=1)}$ **−5.8°C**	
		ΔDPT (m)	ΔSHC (MJ m^{-2})	ΔDPT (m)	ΔSHC (MJ m^{-2})	ΔDPT (m)	ΔSHC (MJ m^{-2})
LINEAR	Linear trend	2.7	706	0.94	281	0.35	167
EARLY	Accelerated warming yrs 6-15	3.6	899	1.19	347	0.35	191
MID	Accelerated warming yrs 21-30	3.1	767	1.11	321	0.35	180
LATE	Accelerated warming yrs 36-45	1.9	532	0.87	254	0.35	147

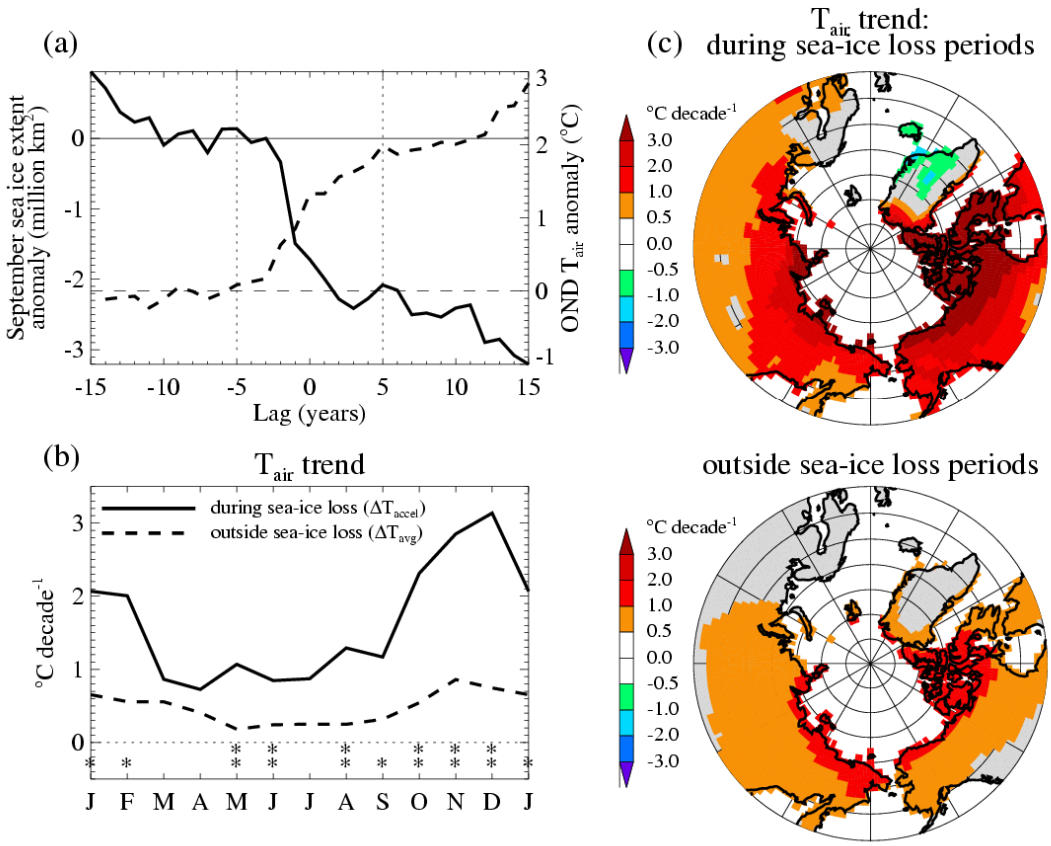

Figure 1: (a) Composite lagged time series of September sea ice extent (solid line) and OND T_{air} (dashed line) over Arctic land area (65°-80°N, 60°-300°E). Composites are centered around the mid-points of the nine rapid sea ice loss events seen in the CCSM3 A1B simulations. Results shown as anomalies from the average of years −10 to −5. (b) Average monthly Arctic land air temperature trends during rapid sea ice loss periods and outside sea ice loss periods. Trend is statistically significant at the 90% (*) and 95% (**) levels. (c) Maps of air temperature trends for OND during and outside abrupt sea ice loss periods.

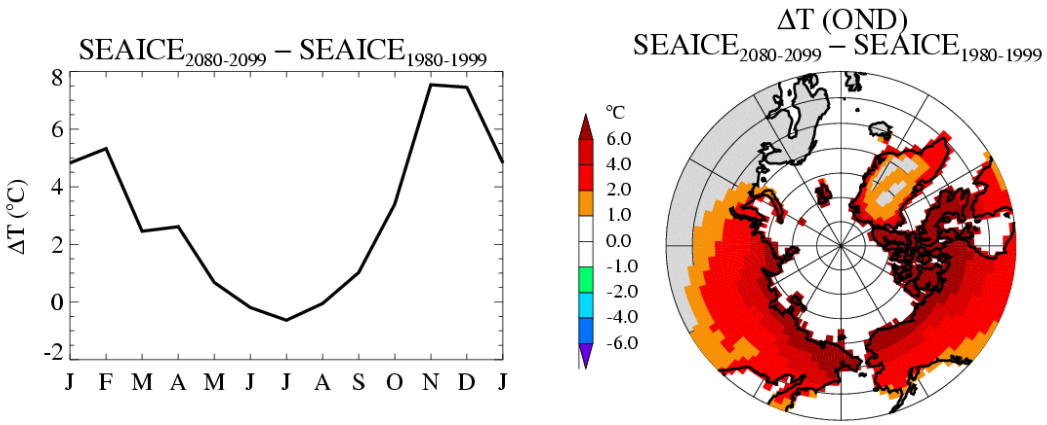

Figure 2: ΔT_{air} between simulation with prescribed 2080-2099 sea-ice conditions obtained from CCSM3 A1B 21st century ensemble and prescribed 1980-1999 sea-ice conditions obtained from CCSM3 20th century ensemble. (a) Monthly ΔT_{air} over western Arctic land (65°-80°N, 60°-300°E). (b) Map of ΔT_{air} for OND.

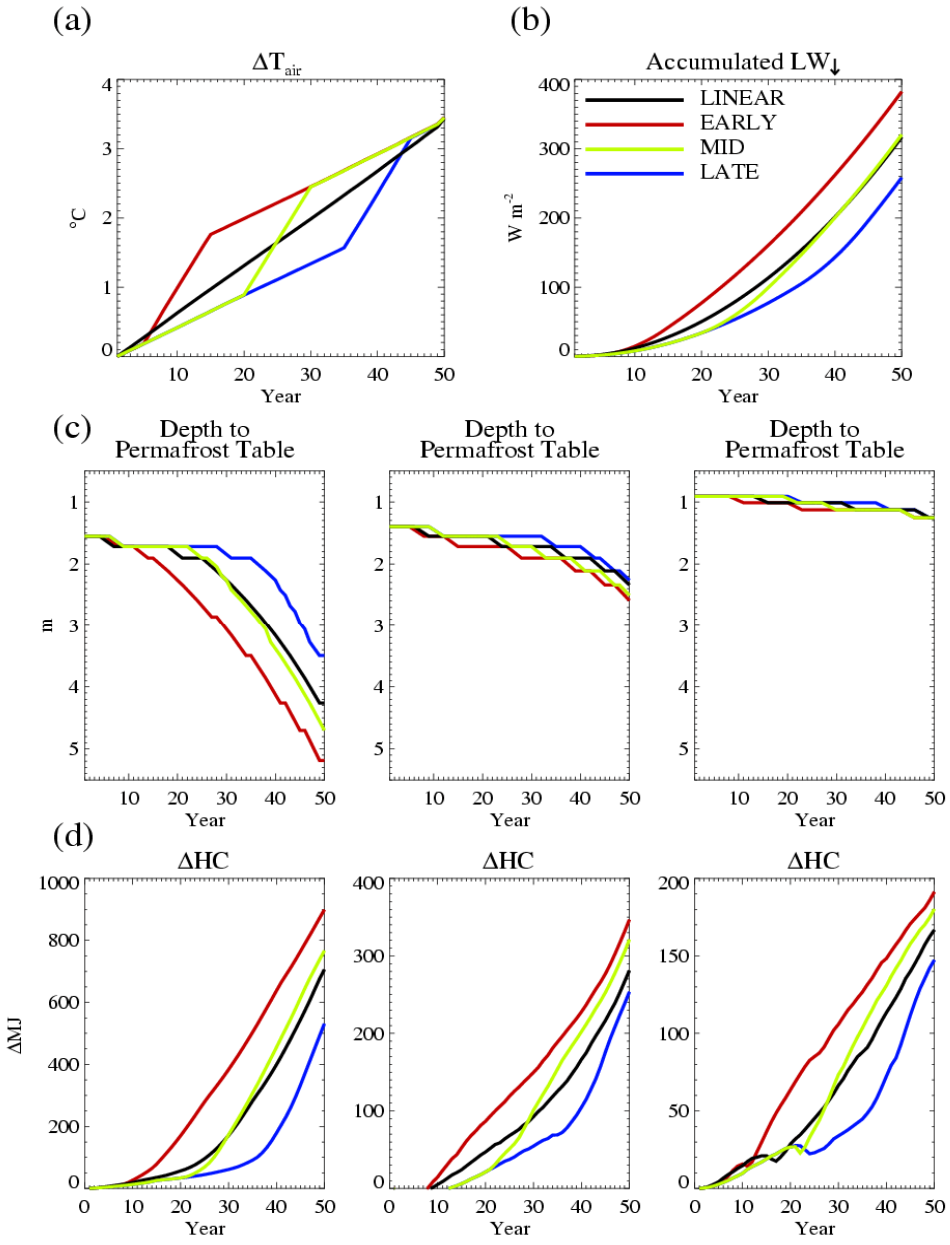

Figure 3: (a) Annual mean T_{air} anomaly time series for the four experiments. Note that monthly air temperature anomalies used in the forced experiments contain the annual cycle structure shown in Fig. 1c. (b) Accumulated LW↓ anomaly time series. (c) Depth to permafrost table (DPT), and (d) change in soil heat content (ΔSHC) for three different initial permafrost states; $\overline{T_{soil}(PT, y=1)} = -0.3°C,\ -1.5°C$, and $-5.8°C$ from left to right. (e) Time series of depth of warming and cooling fronts from LINEAR experiment for warm permafrost case. Location of permafrost and talik are also shown.

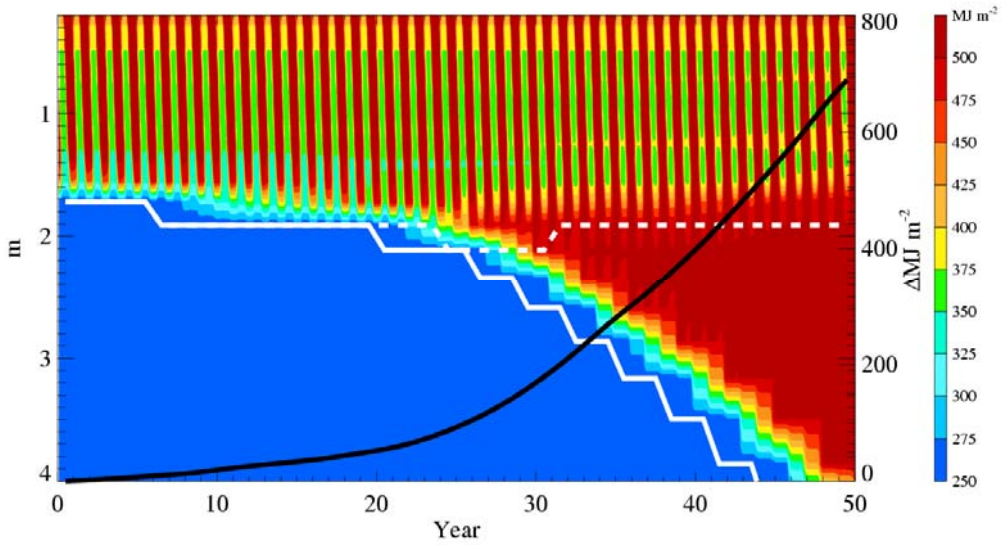

Figure 4: Time series of depth of warming (white solid line) and cooling (white dashed line) fronts from LINEAR experiment for warm permafrost case. Contours indicate SHC. Change in SHC is shown as black line.